14570707, and C 15590786, by a Ground-Based Research Grant for space utilization promoted by the National Space Development Agency of Japan and the Japan Space Forum, and by the Program for Promotion of Fundamental Studies in Health Science of the Organization for Pharmaceutical Safety and Research of Japan.

REFERENCES

1. **Applegate RJ, Cheng CP, and Little WC.** Simultaneous conductance catheter and dimension assessment of left ventricle volume in the intact animal. *Circulation* 81: 638–648, 1990.
2. **Asanoi H, Ishizaka S, Kameyama T, Nozawa T, Miyagi K, and Sasayama S.** Serial reproducibility of conductance catheter volumetry of left ventricle in conscious dogs. *Am J Physiol Heart Circ Physiol* 262: H911–H915, 1992.
3. **Baan J, Jong TT, Kerkhof PL, Moene RJ, van Dijk AD, van der Velde ET, and Koops J.** Continuous stroke volume and cardiac output from intra-ventricular dimensions obtained with impedance catheter. *Cardiovasc Res* 15: 328–334, 1981.
4. **Baan J, van der Velde ET, de Bruin HG, Smeenk GJ, Koops J, van Dijk AD, Temmerman D, Senden J, and Buis B.** Continuous measurement of left ventricular volume in animals and humans by conductance catheter. *Circulation* 70: 812–823, 1984.
5. **Ciagolani OH, Yang XP, Cavasin MA, and Carretero OA.** Increased systolic performance with diastolic dysfunction in adult spontaneously hypertensive rats. *Hypertension* 41: 249–254, 2003.
6. **Feldman MD, Mao Y, Valvano JW, Pearce JA, and Freeman GL.** Development of a multifrequency conductance catheter-based system to determine LV function in mice. *Am J Physiol Heart Circ Physiol* 279: H1411–H1420, 2000.
7. **Francis J, Weiss RM, Wei SG, Johnson AK, and Felder RB.** Progression of heart failure after myocardial infarction in the rat. *Am J Physiol Regul Integr Comp Physiol* 281: R1734–R1745, 2001.
8. **Gawne TJ, Gray KS, and Goldstein RE.** Estimating left ventricular offset volume using dual-frequency conductance catheters. *J Appl Physiol* 63: 872–876, 1987.
9. **Georgakopoulos D and Kass DA.** Estimation of parallel conductance by dual-frequency conductance catheter in mice. *Am J Physiol Heart Circ Physiol* 279: H443–H450, 2000.
10. **Gopakumaran B, Osborn P, Petre JH, and Murray PA.** A new technique to measure and track blood resistivity in intracardiac impedance volumetry. *J Clin Monit* 13: 363–371, 1997.
11. **Hettrick DA, Battocletti JH, Ackmann JJ, Linehan JH, and Waritier DC.** Effects of physical parameters on the cylindrical model for volume measurement by conductance. *Ann Biomed Eng* 25: 126–134, 1997.
12. **Heyen JR, Blasi ER, Nikula K, Rocha R, Daust HA, Frierdich G, Van Vleet JF, De Ciechi P, McMahon EG, and Rudolph AE.** Structural, functional, and molecular characterization of the SHHF model of heart failure. *Am J Physiol Heart Circ Physiol* 283: H1775–H1784, 2002.
13. **Holt BD, Ball N, and Walsh RA.** Invasive hemodynamics and force-frequency relationships in open- versus closed-chest mice. *Am J Physiol Heart Circ Physiol* 273: H2528–H2533, 1997.
14. **Ito H, Takaki M, Yamaguchi H, Tachibana H, and Suga H.** Left ventricular volumetric conductance catheter for rats. *Am J Physiol Heart Circ Physiol* 270: H1509–H1514, 1996.
15. **Kubota T, Mahler CM, McTiernan CF, Wu CC, Feldman MD, and Feldman AM.** End-systolic pressure-dimension relationship of in situ mouse left ventricle. *J Mol Cell Cardiol* 30: 357–363, 1998.
16. **Lapointe N, Blais C Jr, Adam A, Parker T, Sirois MG, Gosselin H, Clement R, and Rouleau JL.** Comparison of the effects of an angiotensin-converting enzyme inhibitor and a vasopeptidase inhibitor after myocardial infarction in the rat. *J Am Coll Cardiol* 39: 1692–1698, 2002.
17. **Litwin SE, Katz SE, Morgan JP, and Douglas PS.** Serial echocardiographic assessment of left ventricular geometry and function after large myocardial infarction in the rat. *Circulation* 89: 345–354, 1994.
18. **Lou E, Fedorak MV, Hill DL, Raso JV, Moreau MJ, and Mahood JK.** Bluetooth wireless database for scoliosis clinics. *Med Biol Eng Comput* 41: 346–349, 2003.
19. **Mills PA, Huetteman DA, Brockway BP, Zwiers LM, Gelsema AJ, Schwartz RS, and Kramer K.** A new method for measurement of blood pressure, heart rate, and activity in the mouse by radiotelemetry. *J Appl Physiol* 88: 1537–1544, 2000.
20. **Mur G and Baan J.** Computation of the input impedances of a catheter for cardiac volumetry. *IEEE Trans Biomed Eng* 31: 448–453, 1984.
21. **Murphy AM, Kogler H, Georgakopoulos D, McDonough JL, Kass DA, Van Eyk JE, and Marban E.** Transgenic mouse model of stunned myocardium. *Science* 287: 488–491, 2000.
22. **Price HL and Ohnishi ST.** Effects of anesthetics on the heart. *Fed Proc* 39: 1575–1579, 1980.
23. **Sato T, Shishido T, Kawada T, Miyano H, Miyashita H, Inagaki M, Sugimachi M, and Sunagawa K.** ESPVR of in situ rat left ventricle shows contractility-dependent curvilinearity. *Am J Physiol Heart Circ Physiol* 274: H1429–H1434, 1998.
24. **Sato T, Shishido T, Miyashita H, Yoshimura R, and Sunagawa K.** Single-beat estimation of end-systolic elastance (E_{es}) in rats (Abstract). *Circulation* 96 *Suppl* I: I-518, 1997.
25. **Shishido T, Hayashi K, Shigemi K, Sato T, Sugimachi M, and Sunagawa K.** Single-beat estimation of end-systolic elastance using bilinearly approximated time-varying elastance curve. *Circulation* 102: 1983–1989, 2000.
26. **Steendijk P, Mur G, Van Der Velde ET, and Baan J.** The four-electrode resistivity technique in anisotropic media: theoretical analysis and application on myocardial tissue in vivo. *IEEE Trans Biomed Eng* 40: 1138–1148, 1993.
27. **Uechi M, Asai K, Osaka M, Smith A, Sato N, Wagner TE, Ishikawa Y, Hayakawa H, Vatner DE, Shannon RP, Homey CJ, and Vatner SF.** Depressed heart rate variability and arterial baroreflex in conscious transgenic mice with overexpression of cardiac $G_s\alpha$. *Circ Res* 82: 416–423, 1998.
28. **Uemura K, Sugimachi M, Shishido T, Kawada T, Inagaki M, Zheng C, Sato T, and Sunagawa K.** Convenient automated conductance volumetric system. *Jpn J Physiol* 52: 497–503, 2002.
29. **Uemura K, Sugimachi M, and Sunagawa K.** Self-calibratable ventricular pressure-volume telemetry system for rats (Abstract). *Circulation* 108 *Suppl* IV: IV-37, 2003.
30. **Vatner SF and Braunwald E.** Cardiovascular control mechanisms in the conscious state. *N Engl J Med* 293: 970–976, 1975.
31. **Wood JW.** Stray-capacitance neutralisation for high-resistance microelectrodes—a simple analysis. *Med Biol Eng Comput* 19: 230–236, 1981.

Effect of Serum Albumin on QRS Wave Amplitude in Patients Free of Heart Disease

Yoshihiro Kudo, MD, Fumiyasu Yamasaki, MD, Hiromi Kataoka, MS, Yoshinori Doi, MD, and Tetsuro Sugiura, MD

We studied 193 patients free of heart disease to determine the relation between QRS amplitude and serum albumin. Although there were no significant differences in echocardiographic indexes between the 2 groups, albumin (35.1 ± 4.3 vs 40.1 ± 3.2 g/L) and colloid osmotic pressure (21 ± 4 vs 24 ± 3 mm Hg) were significantly lower in patients with low voltages compared with those without. Moreover, there was a good relation (r = 0.78) between change in QRS amplitude and change in albumin concentration. ©2005 by Excerpta Medica Inc.

(Am J Cardiol 2005;95:789–791)

From the Departments of Laboratory Medicine and Medicine and Geriatrics, Kochi Medical School, Kochi, Japan. Dr. Sugiura's address is: Department of Laboratory Medicine, Kochi Medical School, Kohasu Oko-cho Nankoku City, Kochi 783-8505, Japan. E-mail: sugiurat@med.kochi-u.ac.jp. Manuscript received August 30, 2004; revised manuscript received and accepted November 18, 2004.

Low voltage is 1 of the electrocardiographic manifestations in patients with pericardial effusion,[1–4] but it is also found in other disorders, including myocardial disease, lung disease, hypothyroidism, and obesity. [5] Serum albumin has been reported to have a direct correlation with QRS amplitude[6]; other investigators found an inverse relation between QRS amplitude and body weight in patients with anasarca.[7] However, as anasarca is frequently associated with decreased albumin concentration, the particular effect of albumin in modulating electrocardiographic voltage is yet to be defined. Accordingly, we designed a study to determine the effect of albumin concentration on QRS wave amplitude in patients free of heart and lung diseases.

• • •

Among 5,766 consecutive patients who were referred to our echocardiography laboratory between January 1, 1998, and December 31, 2001, we investigated 193 clinically stable patients (aged 41 to 95 years) with no history of heart or lung disease and no electrocardiographic, chest radiographic, or echocar-

0002-9149/05/$–see front matter
doi:10.1016/j.amjcard.2004.11.040

TABLE 1 Baseline Characteristics

Variable	Low Voltage: Present (n = 35)	Low Voltage: Absent (n = 158)	P Value
Age (yrs)	70 ± 12	67 ± 10	0.124
Men/women	14/21	69/89	0.835
Body mass index (kg/m^2)	21.5 ± 3.2	22.3 ± 4.1	0.280
Albumin (g/L)	35.1 ± 4.3	40.1 ± 3.2	<0.001
Globulin (g/L)	26.3 ± 6.6	27.1 ± 5.8	0.473
Total protein (g/L)	61.5 ± 8.7	67.2 ± 6.4	<0.001
Colloid osmotic pressure (mm Hg)	21 ± 4	24 ± 3	<0.001
Hematocrit (%)	36.2 ± 4.3	37.7 ± 4.6	0.078

TABLE 2 Echocardiographic Indexes

Variable	Low Voltage: Present (n = 35)	Low Voltage: Absent (n = 158)	P Value
Left ventricular			
Ejection fraction (%)	70 ± 7	70 ± 7	1.000
Diastolic dimension (mm)	43 ± 5	44 ± 4	0.204
Systolic dimension (mm)	26 ± 4	27 ± 4	0.182
Ventricular septum (mm)	9.5 ± 1.1	9.3 ± 1.1	0.332
Posterior wall (mm)	9.5 ± 1.4	9.2 ± 1.1	0.168
Left atrium (mm)	33 ± 5	34 ± 5	0.286

diographic abnormalities. Patients with pericardial effusion or anasarca were not included in this study.

Electrocardiograms were obtained within 24 hours of echocardiography, and R- and S-wave amplitudes were measured directly from the standard 12-lead electrocardiograph to the nearest 0.5 mm using calipers and a magnifying glass. The average of 3 QRS complexes (sum of R and S waves) was determined for each lead. Low voltage was defined as a QRS amplitude <5 mm in all limb leads and/or a QRS amplitude <10 mm in all precordial leads. Low voltage was considered present only after diagnosis by 2 cardiologists who had no knowledge of clinical findings. For patients with low voltage, total QRS wave amplitude was defined as the sum of the R- and S-wave amplitudes in 6 limb leads.

Blood samples were taken within <24 hours of the electrocardiogram. Serum albumin was measured by dye-binding bromcresol green procedure and total protein by the Biuret method using a Hitachi 747 analyzer (Hitachi, Tokyo, Japan). Hypoalbuminemia was defined as <38 g/dl. Colloid osmotic pressure was calculated according to the equation by Nitta et al[8] and Staub et al,[9]: [Colloid osmotic pressure = $a(2.8c + 0.18c^2 + 0.012c^3) + b(0.9c + 0.12c^2 + 0.004c^3)$], where "a" is the albumin fraction, "b" is the globulin fraction, and "c" is total protein (grams per liter). Hematocrit was measured by the red blood cell cumulative pulse height detection method using the Sysmex SE 9000 hematology analyser (Sysmex, Kobe, Japan).

An experienced echocardiographer performed M-mode and 2-dimensional echocardiography with a Toshiba SSH 160A phased-array sector scanner

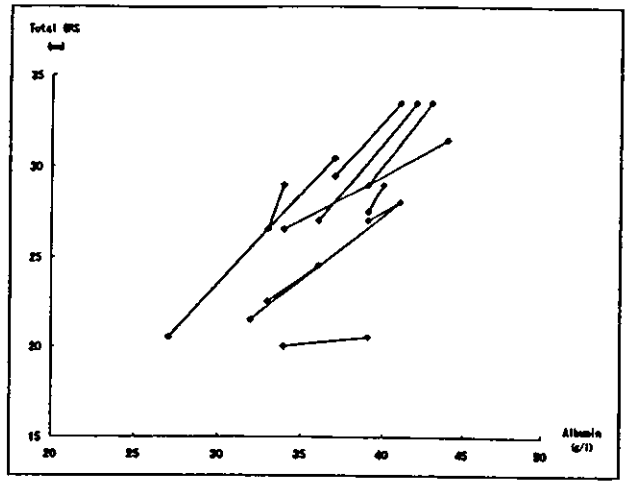

FIGURE 1. Relation of change in total QRS amplitude to change in serum albumin concentration.

(Toshiba, Tokyo, Japan) using a 3.75- or 2.5-MHz transducer. The internal dimension of the left ventricle at end-diastole was measured at the onset of the QRS complex, and the end-systolic dimension was measured at the nadir of septal motion.[10] The thickness of the ventricular septum and posterior wall was measured at the onset of the QRS complex. All classic views were recorded on videotape for subsequent analysis by observers who were unaware of the electrocardiographic data.

Results are reported as mean ± SD. Statistical analysis between the 2 groups was performed by Student's *t* test for continuous variables and Fisher's exact probability test for discrete variables. A paired *t* test was used for paired samples. Regression analysis was used to evaluate the relation between the 2 variables. A p value <0.05 was considered significant.

Among 193 patients, 142 patients were referred to the echocardiographic laboratory to rule out heart disease before operation; 17 patients had connective tissue disease and 34 patients had other noncardiac disorders. Low voltage was detected in 35 patients (18%). Values for albumin and total protein, and colloid osmotic pressure were significantly lower in patients with low voltage compared with those without, but there were no significant differences in the echocardiographic indexes between the 2 groups (Tables 1 and 2). Twenty-seven of 57 patients with hypoalbuminemia had low voltages, whereas 8 of 136 patients without hypoalbuminemia had low voltages. The sensitivity and specificity of low voltages to identify hypoalbuminemia were 47% and 94%, respectively.

In patients with low voltage, there was a fair relation between QRS amplitude and albumin concentration ($r = 0.69$, $p < 0.001$). Follow-up electrocardiography, echocardiography, and serum albumin values were obtained in 11 patients at a mean follow-up of 3.2 ± 2.1 months (0.5 to 6). The serum albumin concentration increased in 9 patients and decreased in 2 patients. Although there were no significant changes in left ventricular diastolic dimension (44 ± 5 vs 44 ± 5 mm), left ventricular systolic dimension (27 ± 6 vs 27 ± 5 mm), septal

thickness (10 ± 1 vs 10 ± 1 mm), and left ventricular posterior wall thickness (10 ± 1 vs 10 ± 1 mm), an increase (decrease) in albumin was accompanied by an increase (decrease) in the total QRS wave amplitude (Figure 1). Moreover, there was a good correlation between the change in total QRS amplitude and the change in albumin concentration ($r = 0.78$, $p = 0.005$).

• • •

The attenuation of QRS wave amplitude is linked to obesity, various lung diseases, and anasarca, whereas augmentation of QRS wave amplitude is associated with a reduction in hematocrit or after hemodialysis.[5–7,11–14] Despite no significant differences in echocardiographic indexes, hematocrit, and body mass index, the serum albumin concentration was significantly lower in patients with low voltages compared with those without. Moreover, low voltage was a highly specific, although not sensitive, electrocardiographic sign of hypoalbuminemia. When the change in albumin concentration and in QRS wave amplitude was assessed, there was a good correlation between these 2 variables. These data indicate that the surface electrocardiographic potentials are attenuated when the resistance of the extracellular space is decreased because of increased extracellular fluid. Thus, serum albumin concentration can affect QRS wave amplitude in patients free of heart and lung diseases.

1. Unverferth DV, Williams TE, Fulkerson PK. Electrocardiographic voltage in pericardial effusion. *Chest* 1979;75:157–160.
2. Spodick DH. The normal and diseased pericardium: current concepts of pericardial physiology, diagnosis and treatment. *J Am Coll Cardiol* 1983;1:240–251.
3. Meyers DG, Bagin RG, Levene JF. Electrocardiographic changes in pericardial effusion. *Chest* 1993;104:1422–1426.
4. Kudo Y, Yamasaki F, Doi T, Doi Y, Sugiura T. Clinical significance of low voltage in asymptomatic patients with pericardial effusion free of heart disease. *Chest* 2003;124:2064–2067.
5. Wagner GS. Marriott's Practical Electrocardiography. 9th Ed. Baltimore: Williams & Wilkins, 1994:176–179.
6. Heaf JG. Albumin-induced changes in the electrocardiographic QRS complex. *Am J Cardiol* 1985;55:1530–1533.
7. Madias JE, Bazaz R, Agarwal H, Win M, Medepalli L. Anasarca-mediated attenuation of the amplitude of electrocardiogram complexes: a description of a heretofore unrecognized phenomenon. *J Am Coll Cardiol* 2001;38:756–764.
8. Nitta S, Ohnuki T, Ohkuda K, Nakada T, Staub NC. The corrected protein equation to estimate plasma colloid osmotic pressure and its development on a nomogram. *Tohoku J Exp Med* 1981;135:43–49.
9. Staub NC. Pathophysiology of pulmonary edema. In: Staub NC, Taylor AE, eds. Edema. New York: Raven Press, 1984:719–746.
10. Henry WL, Gardin JM, Ware JH. Echocardiographic measurements in normal subjects from infancy to old age. *Circulation* 1980;62:1054–1060.
11. Rudy Y, Plonsey R, Liebman J. The effects of variations in conductivity and geometrical parameters on the electrocardiogram, using an eccentric spheres model. *Circ Res* 1979;44:104–111.
12. Rosenthal A, Resticaux NJ, Feig SA. Influence of acute variations in hematocrit on the QRS complex of the Frank electrocardiogram. *Circulation* 1971;44:456–465.
13. Ishikawa K, Nagasawa T, Shimada H. Influence of hemodialysis on electrocardiographic wave forms. *Am Heart J* 1979;97:5–11.
14. Dudley SC, Baumgarten CM, Ornato JP. Reversal of low voltage and infarction pattern of the surface electrocardiogram after renal hemodialysis for pulmonary edema. *J Electrocardiol* 1990;23:341–345.

FEBS Lett in press

Acetylcholine From Vagal Stimulation Protects Cardiomyocytes Against Ischemia and Hypoxia Involving Additive Nonhypoxic Induction of HIF-1α

Yoshihiko Kakinuma, Motonori Ando, *Masanori Kuwabara, Rajesh G Katare,
#Koji Okudela, +Masanobu Kobayashi, Takayuki Sato

Department of Cardiovascular Control, *Department of Medicine and Geriatrics,
Kochi Medical School, Nankoku, Japan.
#Department of Pathology, Division of Cellular Pathobiology,
Yokohama City University Graduate School of Medicine, Yokohama, Japan.
+Division of Cancer Pathobiology, Institute for Genetic Medicine, Hokkaido University, Sapporo, Japan

Correspondence:Yoshihiko Kakinuma, M.D., Ph.D. Department of Cardiovascular Control Kochi Medical SchoolNankoku, 783-8505, Japan
FAX: +81-88-880-2310 TEL:+81-88-880-2587 E-mail:kakinuma@med.kochi-u.ac.jp

ABSTRACT

Electrical stimulation of the vagal efferent nerve improves the survival of myocardial infarcted rats. However, the mechanism for this beneficial effect is unclear. We investigated the effect of acetylcholine (ACh) on HIF-1α using rat cardiomyocytes under normoxia and hypoxia. ACh posttranslationally regulated HIF-1α and increased its protein level under normoxia. ACh increased Akt phosphorylation, and wortmannin or atropine blocked this effect. Hypoxia-induced caspase-3 activation and mitochondrial membrane potential collapse were prevented by ACh. Dominant-negative HIF-1α inhibited the cell protective effect of ACh. In acute myocardial ischemia, vagal nerve stimulation increased HIF-1α expression and reduced the infarct size. These results suggest that ACh and vagal stimulation protect cardiomyocytes through the PI3K/Akt/HIF-1α pathway.

Key words: acetylcholine, ischemia, apoptosis, protein kinases

1. Introduction

The prognosis of patients with chronic heart failure remains poor, due to progressive remodeling of the heart and lethal arrhythmia. Acute ischemia or hypoxia causes loss of cardiomyocytes, followed by remodeling in the chronic phase. Although various therapeutic approaches have been introduced, including implantable defibrillators [1], a more effective modality of therapy has been anticipated for several years. A recent animal study by Li et al. demonstrated that vagal nerve stimulation prevented ventricular remodeling after myocardial infarction, suggesting a novel therapeutic strategy against heart failure [2]. Furthermore, Krieg et al. reported that acetylcholine (ACh) has a cardioprotective effect [3]. Although nitric oxide (NO) is supposed to be a major signaling molecule induced by ACh, a mechanism for the beneficial effect of vagal nerve stimulation on cardiomyocytes remains to be clarified. To investigate this mechanism, we hypothesized that vagal stimulation or ACh directly triggers a cell survival signal that is subsequently amplified and leads to protection of the cardiomyocytes from acute ischemic conditions, and that this effect of ACh, if continued, could be responsible for chronic cardioprotection.

In the present study, we focused on demonstrating the cellular action of ACh through hypoxia-inducible factor (HIF)-1α. HIF-1α is a transcription factor that is important for cell survival under hypoxia. HIF-1α activates the expression of many genes indispensable for cell survival [4,5]. Under normoxia, the HIF-1α protein level is very low, due to proteasomal degradation through with von Hippel-Lindau tumor suppressor protein (VHL). However, HIF-1α escapes from this degradation under hypoxia, and this is recognized as the hypoxic pathway [6,7]. Recently, it was revealed that HIF-1α can be also induced via a nonhypoxic pathway by angiotensin II [8,9]. Taken together, it is conceivable that HIF-1α induction is one of the adaptation processes to hypoxia and ischemia, and that additional induction of HIF-1α during ischemia via a nonhypoxic pathway could provide further cardioprotection.

Therefore, we investigated the direct effects of ACh on survival signaling in cardiomyocytes and of vagal stimulation on hearts. The results suggest that ACh and vagal stimulation protect cardiomyocytes from acute hypoxia and ischemia via additional HIF-1α protein induction through a nonhypoxic pathway.

2. Materials and Methods

2.1. Cell Culture

To examine the effect of ACh on cardiomyocytes, H9c2 cells as well as primary cardiomyocytes isolated from neonatal rats were used. H9c2 cells, which are frequently used to investigate signal

transduction and channels in rat cardiomyocytes, are derived from rat embryonic ventricular cardiomyocytes. H9c2 cells were incubated in DMEM containing 10% FBS and antibiotics. Primary cardiomyocytes were isolated from 2-3-day-old neonatal WKY rats and incubated in DMEM/Ham F-12 containing 10% FBS. HEK293 cells and HeLa cells cultured in DMEM containing 10% FBS were also used.

2.2. Western Blot Analysis

H9c2 cells and primary cardiomyocytes were treated with 1 mM ACh to evaluate expression of HIF-1a protein under normoxia or with 1 mM S-nitroso-N-acetylpenicillamine (SNAP) to study the signal transduction. To investigate the signal transduction, H9c2 cells were pretreated with a PI3K inhibitor, (wortmannin; 300 nM), a muscarinic receptor, (atropine; 1 mM), a transcriptional inhibitor, (actinomycin D; 0.5 μg/ml) or a protein synthesis inhibitor, (cycloheximide; 10 μg/ml), followed by ACh treatment. Cell lysates were mixed with a sample buffer, fractionated by 10% SDS-PAGE and transferred onto membranes. The membranes were incubated with primary antibodies against HIF-1a (Santa Cruz Biotechnology, Santa Cruz, California, USA), Akt and phospho-Akt (Cell Signaling Technology, Beverly, Massachusetts, USA), and α-tubulin (Lab Vision, Fremont, California, USA), and then reacted with an HRP-conjugated secondary antibody (BD Transduction Laboratories, San Diego, California, USA). Positive signals were detected with an enhanced chemiluminescence system (Amersham, Piscataway, New Jersey, USA). In each study, the experiments were performed in duplicate and repeated 3-5 times (n=3-5). Representative data are shown.

2.3. MTT Activity Assay

To evaluate the effects of hypoxia and ACh on the mitochondrial function of cardiomyocytes, we measured 3-(4,5-dimethylthiazol-2-yl)-2,5-diphenyl tetrazolium bromide (MTT) reduction activity in H9c2 or HEK293 cells under hypoxia (1% oxygen concentration), in the presence or absence of ACh. The cells were pretreated with 1 mM ACh for 12 hours, and then subjected to hypoxia for 12 hours. At 4 hours before sampling, the MTT reagents were added to the culture and incubated.

2.4. Caspase-3 Activity Assay

Caspase-3 activity was measured using a CPP32/Caspase-3 Fluorometric Protease Assay Kit, (CHEMICON INTERNATIONAL, Temecula, California, USA). Hypoxia-treated H9c2 cells with or without 1 mM ACh pretreatment were lysed and the cytosolic extract was added to the caspase-3 substrate. A fluorometer equipped with a 400-nm excitation filter and 505-nm emission filter was used to measure the samples.

2.5. DePsipher Assay

To examine the effects of hypoxia and ACh on the mitochondrial electrochemical gradient, we analyzed cardiomyocytes using a DePsipher™ Mitochondrial Potential Assay Kit (Trevigen, Gaithersburg, Maryland, USA). Apoptotic cells, which undergo mitochondrial membrane potential collapse cannot accumulate the DePsipher reagent in their mitochondria. As a result, apoptotic cells show decreased red fluorescence in their mitochondria, and the reagent remains in the cytoplasm as a green fluorescent monomer. Therefore, apoptotic cells were easily differentiated from healthy cells, which showed more red fluorescence.

2.6. Evaluation of NO production

NO production was measured using the 4,5 diaminofluoresceindiacetate (DAF-2DA; Alexis, Lausen, Switzerland) fluorometric NO detection system as previously reported [10]. The intensity of the DAF-2DA green fluorescence in ACh-treated cells was measured and compared with that in non-treated cells (λ Ex. 492 nm; λ Em. 515 nm).

2.7. Transfection

To investigate the direct contribution of Akt phosphorylation to HIF-1a stabilization or that of HIF-1a to the ACh effect, HEK293 cells were transfected with an expression vector for wild-type Akt (wt Akt), dominant-negative Akt (dn Akt), wild-type HIF-1α (wt HIF-1α) or dominant-negative HIF-1α (dn HIF-1α), using Effectene (Qiagen, Valencia, California, USA) according to the manufacture's protocol. The Akt vectors were generous gifts from by Dr. K. Okudela (Yokohama City University, Kanagawa, Japan) [11], while the HIF-1α vectors were kindly provided by Dr. M. Kobayashi (Hokkaido University, Sapporo, Japan) [12]. After transfection, HEK293 cells were pretreated with 1 mM ACh for 12 hours, followed by evaluating the HIF-1α protein level or by hypoxia for 12 hours and MTT activity in each group was evaluated. As a control, cells were transfected with a vector for green fluorescent protein (GFP).

2.8. RT-PCR

Total RNA was isolated from H9c2 cells according to a modified acid guanidinium-phenol-chloroform method using an RNA isolation kit (ISOGEN; Nippon Gene, Tokyo, Japan), and reverse-transcribed to obtain a first-strand cDNA. This first-strand cDNA was amplified by specific primers for HIF-1a, and the PCR products were fractionated by electrophoresis.

2.9. Vagal Nerve Stimulation in Myocardial Ischemia

Left ventricular myocardial ischemia (MI) was performed by 3 hours of left coronary artery (LCA) ligation in anesthetized 9-week-old male Wistar rats

under artificial ventilation previously described [2]. Sham-operated (control) rats did not undergo LCA ligation. For vagal nerve stimulation (VS), the right vagal nerve in the neck was isolated and cut. Only the distal end of the vagal nerve was stimulated in order to exclude the effects of the vagal afferent. The electrode was connected to an isolated constant voltage stimulator. VS was performed from 1 min before the LCA ligation until 3 hours afterwards, using 0.1 ms pulses at 10 Hz (MI-VS). The electrical voltage of the pulses was adjusted to obtain a 10% reduction in the heart rate before LCA ligation, but VS (MI-VS) was not associated with any blood pressure reduction during the experiments, compared with MI. At the end of the experiments, the rats were either injected with 2 ml of 2% Evans blue dye via the femoral vein to measure the risk area followed by determination of the infarct size with 2% triphenyl tetrazolium chloride (TTC) staining or the heart was excised for protein isolation and subsequent western blotting to detect HIF-1a protein. The percentage of the infarcted area of the left ventricle (LV) was calculated as the ratio of the infarcted area to the risk area.

2.10. Densitometry

The western blotting data were analyzed using Kodak 1D Image Analysis Software (Eastman Kodak Co., Rochester, New York, USA).

2.11. Statistics

The data were presented as means ± S.E. The mean values between two groups were compared by the unpaired Student's t test. Differences among data were assessed by ANOVA for multiple comparisons of results. Differences were considered significant at $P<0.05$.

3. Results

3.1. Posttranslational Regulation of HIF-1α by ACh through a Nonhypoxic Pathway

ACh (1 mM) increased HIF-1α protein expression in H9c2 cells under normoxia (Fig. 1A). ACh increased NO production, as evaluated by DAF-2DA (Figure 1B), suggesting that NO is involved in the signal transduction of HIF-1a induction. Actinomycin D (0.5 μg/ml; Figs. 2A, 2B) and cycloheximide (10 μg/ml; Fig. 2C) did not decrease the HIF-1α level under normoxia, suggesting that HIF-1α degradation is regulated by ACh. Furthermore, ACh increased HIF-1 α level in primary cardiomyocytes without reducing their beating rate (Fig. 3). Since H9c2 cells did not beat, these results suggest that HIF-1α induction is independent of the heart rate-decreasing effect of ACh.

3.2. Akt Phosphorylation by ACh

ACh had no effect on the total Akt protein level, but increased Akt phosphorylation (Fig. 4A) as effectively as SNAP (data not shown). The ACh-induced Akt phosphorylation was inhibited by atropine in a dose-dependent manner (Fig. 4B). ACh-induced Akt phosphorylation and its inhibition by atropine were also observed in rat primary cardiomyocytes (Fig. 4C).

3.3. PI3K/Akt Pathway for HIF-1α induction by ACh

Wortmannin completely inhibited the ACh-induced Akt phosphorylation (Fig. 4D), in clear contrast to the data in Fig. 4A. Furthermore, it also attenuated the HIF-1α induction by ACh (Fig. 4E). To elucidate the contribution of Akt phosphorylation to HIF-1α protein level in normoxia, dn Akt was introduced into HEK293 cells, and found to partially inhibit the HIF-1α induction by ACh (Fig. 4F).

3.4. Effect of ACh on Apoptosis during Hypoxia

The DePsipher assay clearly showed that hypoxia (1% oxygen concentration) for 12 hours caused mitochondrial membrane potential collapse leading to cell death, and that 1 mM ACh inhibited this collapse in H9c2 cells (Fig. 5A). ACh attenuated the decrease in MTT activity caused by 12 hours of hypoxia in H9c2 cells (Fig. 5B; 103.4±0.8% in ACh+hypoxia vs. 56.6±0.7% in hypoxia, $p<0.01$, n=8) and HEK293 cells ($p<0.01$ vs. hypoxia). The caspase-3 activity was increased by hypoxia in H9c2 cells, and pretreatment with 1 mM ACh inhibited this increase (Fig. 5C; 128±2% in hypoxia vs. 90±2% in ACh+hypoxia, $p<0.01$, n=4). To elucidate the dependency of the ACh-induced protective effect on HIF-1α, dn HIF-1α was transfected into HEK293 cells, followed by ACh pretreatment and then hypoxia. It was found that dn HIF-1α inhibited the protective effect of ACh from hypoxia (Fig. 5D; 115.1±1.2% in wt HIF-1α and 111.8±1.8% in GFP vs. 59.0±3.4% in dn HIF-1α, $p<0.05$, n=10), suggesting that HIF-1α induction by ACh is partially responsible for the protective effect.

3.5. Effect of Vagal Stimulation on HIF-1a in Myocardial Ischemia

To evaluate the significance of ACh for cardioprotection in vivo, the vagal nerve was stimulated prior to the myocardial ischemia. Histological analysis demonstrated a tendency for the infarcted area from the vagal nerve-stimulated (MI-VS) hearts to be smaller than that from non-stimulated (MI) hearts (31.5±4.6% in MI-VS vs. 40.9±2.5% in MI, n=3), even though the risk areas (non-perfused areas) were comparable (Fig. 6A; 59.2±1.0% in MI-VS vs. 53.7±1.0% in MI, n=3). In the MI-VS hearts, the HIF-1α protein level was further elevated compared to that in the MI hearts (Fig. 6B; 244±24% in MI-VS vs. 112±1% in MI, n=3). These results suggest that vagal nerve stimulation in the ischemic heart activates both the hypoxic and nonhypoxic pathways of HIF-1α

induction, resulting in increased induction of HIF-1a.

3.6. Nonhypoxic Induction of HIF-1α in Other Cells

The observed ACh-mediated HIF-1α induction was not limited to H9c2 or primary cultured cardiomyocytes, but also found in several other types of cell lines, including HEK293, and HeLa cells (Figure 7). Since these cells did not beat spontaneously, the results suggest that the system of ACh-mediated HIF-1α induction is not only independent of the beating rate of cardiomyocytes, but also a generally conserved system in cells.

4. Discussion

Cardioprotective Action by ACh and Vagal Stimulation via the Muscarinic Receptor

Using animal models, several studies have shown that accentuated antagonism against the sympathetic nervous system is a major mechanism for the beneficial effect of vagal tone on the ischemic heart [13]. Although ACh was involved in triggering preconditioning mechanisms in an ischemia-reperfusion model [3], it remained unclear whether vagal nerve stimulation in acute ischemia or hypoxia followed these mechanisms. In the present study, we have disclosed that ACh possesses a protective effect on cardiomyocytes. In rat cardiomyocytes, ACh triggered a sequence of survival signals through Akt that eventually induced HIF-1α, inhibited the collapse of the mitochondrial membrane potential and decreased caspase-3 activity, thereby leading to the survival of cardiomyocytes under hypoxia. Furthermore, our results suggest ACh exerts this action through Akt in other cells. The current study therefore provides another insight into the cellular mechanism for the cardioprotective effects of ACh and vagal stimulation.

Signaling Pathway of ACh via PI3K/Akt and Antiapoptotic Effects of ACh

Since previous studies demonstrated that a PI3K inhibitor greatly reduced HIF-1α induction in heart and renal cells [14,15] and a few studies have reported that MAP kinase is activated through ACh, we focused on the PI3K/Akt pathway, one of the important cell survival signaling pathways [16], and found that ACh directly activated Akt phosphorylation via PI3K. PI3K/Akt signaling has been reported to have an antiapoptotic activity through various features, such as inhibition of Bad-binding to Bcl-2, caspase 9, Fas and glycogen synthetase kinase-3 [17,18]. These facts imply a definite involvement of Akt activation in cell survival. As shown using dn HIF-1α, ACh inhibited hypoxia-induced cell death through HIF-1α induction via Akt phosphorylation. These results indicate that ACh actually protects cardiomyocytes from hypoxia at the cellular level.

Additional Induction of HIF-1α by ACh and Vagal Stimulation

HIF-1α regulates the transcriptional activities of very diverse genes involved in cell survival and is itself regulated at the posttranslational level by VHL [4,6,7]. Recent studies have shown that HIF-1α is also regulated through a nonhypoxic pathway involving angiotensin II, TNF-α and NO [8,9,19,20]. Therefore, it is speculated that cardiomyocytes possess a similar system for regulating HIF-1α through ACh, independent of the oxygen concentration. Induction of HIF-1α is a powerful cellular response against hypoxia, and further increases in its expression by other pathways may be beneficial. The present results indicate that the significance of ACh or vagal nerve stimulation in hypoxic stress can be attributed to additional HIF-1α induction through dual induction pathways, i.e., hypoxic and nonhypoxic pathways.

The present study has revealed that ACh-mediated HIF-1α induction is widely conserved in other cells. Consistent with a previous report [10], the current results suggest that NO is produced by ACh. According to a report that NO attenuates the interaction between pVHL and HIF-1α through inhibiting PHD activity [21], it is possible that ACh may increase the HIF-1α protein level through NO. Recent studies conducted by Krieg et al. and Xi et al., have provided supportive data compatible with our results [3,22], while another study by Hirota et al. also revealed a nonhypoxic pathway for HIF-1α induction by ACh in a human kidney-derived cell line [23].

The signaling pathway of the muscarinic receptor has been studied extensively, and many pathways are involved in its specific biological effects. Therefore, possible involvement of other pathways in the nonhypoxic induction of HIF-1α cannot be excluded. However, it was demonstrated that dn Akt and dn HIF-1α decreased the effect of ACh. Consistent with a recent study [24], we have revealed that ACh or vagal stimulation protects cardiomyocytes in the acute phase. This observation suggests that the protective effect in the acute phase may result in inhibition of cardiac remodeling in the chronic phase, since vagal stimulation produces additional HIF-1α induction through a nonhypoxic pathway, which increases cell survival.

Acknowledgement

This study was supported by a Health and Labor Sciences Research Grant (H15-PHYSI-001) for Advanced Medical Technology from the Ministry of Health, Labor, and Welfare of Japan.

References

1. Julian D.G, Camm A.J., Frangin G, Janse M.J., Munoz A., Schwartz P.J., Simon P. (1997) Randomised trial of effect of amiodarone on mortality

in patients with left-ventricular dysfunction after recent myocardial infarction: EMIAT. European Myocardial Infarct Amiodarone Trial Investigators. *Lancet* 349, 667-674.
2. Li M., Zheng C., Sato T., Kawada T., Sugimachi M., Sunagawa K. (2004) Vagal nerve stimulation markedly improves long-term survival after chronic heart failure in rats. *Circulation* 109, 120-124.
3. Krieg T., Qin Q., Philipp S., Alexeyev M.F., Cohen M.V., Downey J.M. (2004) Acetylcholine and bradykinin trigger preconditioning in the heart through pathway that includes Akt and NOS. *Am. J. Physiol. Heart Circ. Physiol.* 287, H2606-H2611.
4. Semenza G.L. (2003) HIF-1, O(2), and the 3 PHDs: how animal cells signal hypoxia to the nucleus. *Cell* 107, 1-3.
5. Kakinuma Y., Miyauchi T., Yuki K., Murakoshi N., Goto K., Yamaguchi I. (2001) Novel molecular mechanism of increased myocardial endothelin-1 expression in the failing heart involving the transcriptional factor hypoxia-inducible factor-1a induced for impaired myocardial energy metabolism. *Circulation* 103, 2387–2394.
6. Maxwell P.H., Wiesener M.S., Chang G.W., Clifford S.C., Vaux E.C., Cockman M.E., Wykoff C.C., Pugh C.W., Maher E.R., Ratcliffe P.J. (1999) The tumour suppressor protein VHL targets hypoxia-inducible factors for oxygen-dependent proteolysis. *Nature* 399, 271-275.
7. Min J.H., Yang H., Ivan M., Gertler F., Kaelin W.G. Jr., Pavletich N.P. (2002) Structure of an HIF-1alpha -pVHL complex: hydroxyproline recognition in signaling. *Science* 296, 1886-1889.
8. Page E.L., Robitaille G.A., Pouyssegur J., Richard D.E. (2002) Induction of hypoxia-inducible factor-1alpha by transcriptional and translational mechanisms. *J. Biol. Chem.* 277, 48403-48409.
9. Richard D.E., Berra E., Pouyssegur J. (2000) Nonhypoxic pathway mediates the induction of hypoxia-inducible factor 1alpha in vascular smooth muscle cells. *J. Biol. Chem.* 275, 26765-26771.
10. Zanella B., Calonghi N., Pagnotta E., Masotti L., Guarnieri C. (2002) Mitochondrial nitric oxide localization in H9c2 cells revealed by confocal microscopy. *Biochem. Biophys. Res. Commun.* 290, 1010-1014.
11. Okudela K., Hayashi H., Ito T., Yazawa T., Suzuki T., Nakane Y., Sato H., Ishi H., KeQin X., Masuda A., Takahashi T., Kitamura H. (2004) K-ras gene mutation enhances motility of immortalized airway cells and lung adenocarcinoma cells via Akt activation: possible contribution to non-invasive expansion of lung adenocarcinoma. *Am. J. Pathol.* 164, 91-100.
12. Chen J., Zhao S., Nakada K., Kuge Y., Tamaki N., Okada F., Wang J., Shindo M., Higashino F., Takeda K., Asaka M., Katoh H., Sugiyama T., Hosokawa M., Kobayashi M. (2004) Dominant-negative hypoxia-inducible factor-1 alpha reduces tumorigenicity of pancreatic cancer cells through the suppression of glucose metabolism. *Am. J. Pathol.* 162, 1283-1291.
13. Du X.J., Dart A.M., Riemersma R.A., Oliver M.F. (1990) Failure of the cholinergic modulation of norepinephrine release during acute myocardial ischemia in the rat. *Circ. Res.* 66, 950-956.
14. Kim C.H., Cho Y.S., Chun Y.S., Park J.W., Kim M.S. (2002) Early expression of myocardial HIF-1alpha in response to mechanical stresses: regulation by stretch-activated channels and the phosphatidylinositol 3-kinase signaling pathway. *Circ. Res.* 90, e25-e33.
15. Sandau K.B., Zhou J., Kietzmann T., Brune B. (2001) Regulation of the hypoxia-inducible factor 1alpha by the inflammatory mediators nitric oxide and tumor necrosis factor-alpha in contrast to desferroxamine and phenylarsine oxide. *J. Biol. Chem.* 276, 39805-39811.
16. Vanhaesebroeck B., Alessi D.R. (1999) The regulation and activities of the multifunctional serine/threonine kinase Akt/PKB. *Exp. Cell Res.* 253, 210-229.
17. Kennedy S.G., Wagner A.J., Conzen S.D., Jordan J., Bellacosa A., Tsichlis P.N., Hay N. (1997) The PI3-kinase/Akt signaling pathway delivers an anti-apoptotic signal. *Genes Dev.* 11, 701-713.
18. Cross D.A., Alessi D.R., Cohen P., Andjelkovich M., Hemmings B.A. (1995) Inhibition of glycogen synthase kinase-3 by insulin mediated by protein kinase B. *Nature* 378, 785-789.
19. Zhou J., Schmid T., Brune B. (2003) Tumor necrosis factor-alpha causes accumulation of a ubiquitinated form of hypoxia inducible factor-1alpha through a nuclear factor-kappaB-dependent pathway. *Mol. Biol. Cell* 14, 2216-2225.
20. Sandau K.B., Fandrey J., Brune B. (2001) Accumulation of HIF-1alpha under the influence of nitric oxide. *Blood* 97, 1009-1015.
21. Metzen E., Zhou J., Jelkmann W., Fandrey J., Brune B. (2003) Nitric oxide impairs normoxic degradation of HIF-1alpha by inhibition of prolyl hydroxylases. *Mol. Biol. Cell* 14, 3470-3481.
22. Xi L., Taher M., Yin C., Salloum F., Kukreja R.C. (2004) Cobalt chloride induces delayed cardiac preconditioning in mice through selective activation of HIF-1{alpha} / AP-1 and iNOS Signaling. *Am. J. Physiol. Heart. Circ. Physiol.* 287, H2369-H2375.
23. Hirota K., Fukuda R., Takabuchi S., Kizaka-Kondoh S., Adachi T., Fukuda K., Semenza G.L. (2004) Induction of hypoxia-inducible factor 1 activity by muscarinic acetylcholine receptor signaling. *J. Biol. Chem.* 279, 41521-41528.
24. Wang H., Yu M., Ochani M., Amella C.A., Tanovic M., Susarla S., Li J.H., Wang H., Yang H., Ulloa L., Al-Abed Y., Czura C.J., Tracey K.J. (2003) Nicotinic acetylcholine receptor alpha7 subunit is an essential regulator of inflammation. *Nature* 421, 384-388.

Figure legends

Figure 1

HIF-1a is induced by ACh in rat cardiomyocytes even under normoxia.

A. After treatment of H9c2 cells with 1 mM ACh for 8 hours, the HIF-1a protein level is increased (# $p<0.05$ vs. control, n=4). B. ACh (1 mM) increases the intensity of DAF-2DA fluorescence (# $p<0.01$ vs. control, n=3).

Figure 2

HIF-1α induction by ACh is posttranslationally regulated in rat cardiomyocytes under normoxia.

A. The HIF-1α protein level in H9c2 cells in the presence of 0.5 μg/ml of actinomycin D is increased by 1 mM ACh to a comparable level to

that in the absence of actinomycin D (N.S., not significant, n=3). B. Actinomycin D does not decrease the HIF-1α mRNA level, as evaluated by RT-PCR. C. Cycloheximide (10 μg/ml) does not affect the HIF-1α protein level (n=3).

Figure 3
Rat primary cultured cardiomyocytes show comparable HIF-1α induction by 1 mM ACh to that in H9c2 cells (# $p<0.05$ vs. control, n=3).

Figure 4
Akt is activated by ACh in rat cardiomyocytes, leading to HIF-1α induction.
A. Akt phosphorylation in H9c2 cells is rapidly increased by 1 mM ACh (# $p<0.05$ vs. baseline, n=4), whereas the total protein level of Akt remains unaffected. B. The ACh-induced increase in Akt phosphorylation is blocked by 1 mM atropine (# $p<0.05$ vs. 0 μM atropine, n=3). C. ACh (1 mM) also increases Akt phosphorylation in rat primary cardiomyocytes (# $p<0.05$ vs. baseline, n=3), and atropine blocks this effect. D. Pretreatment with 300 nM wortmannin completely inhibits ACh-induced Akt phosphorylation in H9c2 cells (N.S., not significant, n=3). E. Wortmannin (300 nM) also inhibits HIF-1α induction by ACh (# $p<0.05$ vs. wortmannin (+), n=3). Each figure shows a representative result from 3 independently performed experiments (n=3). F. In contrast to wt Akt, HIF-1α induction y ACh is blocked by dn Akt in HEK293 cells (n=4).

Figure 5
Collapse of the mitochondrial membrane potential in rat cardiomyocytes under hypoxia is attenuated by ACh pretreatment.
A. Hypoxia decreases the mitochondrial membrane potential in H9c2 cells within 12 hours. Red spots are decreased by hypoxia, whereas pretreatment with 1 mM ACh for 12 hours inhibits this effect. B. Pretreatment with 1 mM ACh inhibits the decrease in MTT reduction activity induced by 12 hours of hypoxia not only in H9c2 cells (# $p<0.01$ vs. hypoxia, n=8) but also in HEK293 cells (* $p<0.01$ vs. hypoxia, n=8). C. Hypoxia increases caspase-3 activity, whereas pretreatment with 1 mM ACh inhibits this effect (# $p<0.01$ vs. hypoxia, n=3). D. In contrast to wt HIF-1α or GFP, dn HIF-1α alone decreases the MTT activity under hypoxia after ACh treatment (# $p<0.01$ vs. wt and GFP, * $p<0.05$ vs. non-transfection, n=10).

Figure 6
Vagal nerve stimulation decreases infarcted area with increased HIF-1a expression.
A. A quantitative analysis reveals comparable non-perfused areas in both vagal-stimulated (MI-VS) and non-stimulated (MI) hearts, whereas the infarcted area identified by TTC staining is smaller in the MI-VS heart than in the MI heart. B. HIF-1α induction in the ischemic heart is increased by vagal stimulation (MI-VS) compared with that in ischemia alone (MI) (#, $p<0.01$ vs. MI) (n=3).

Figure 7
HIF-1a is induced by ACh under normoxia in other cells.
ACh (1 mM) increases HIF-1a protein level in HEK293 and HeLa cells (n=3 each) under normoxia.

Kakinuma Y et al
Figure 1

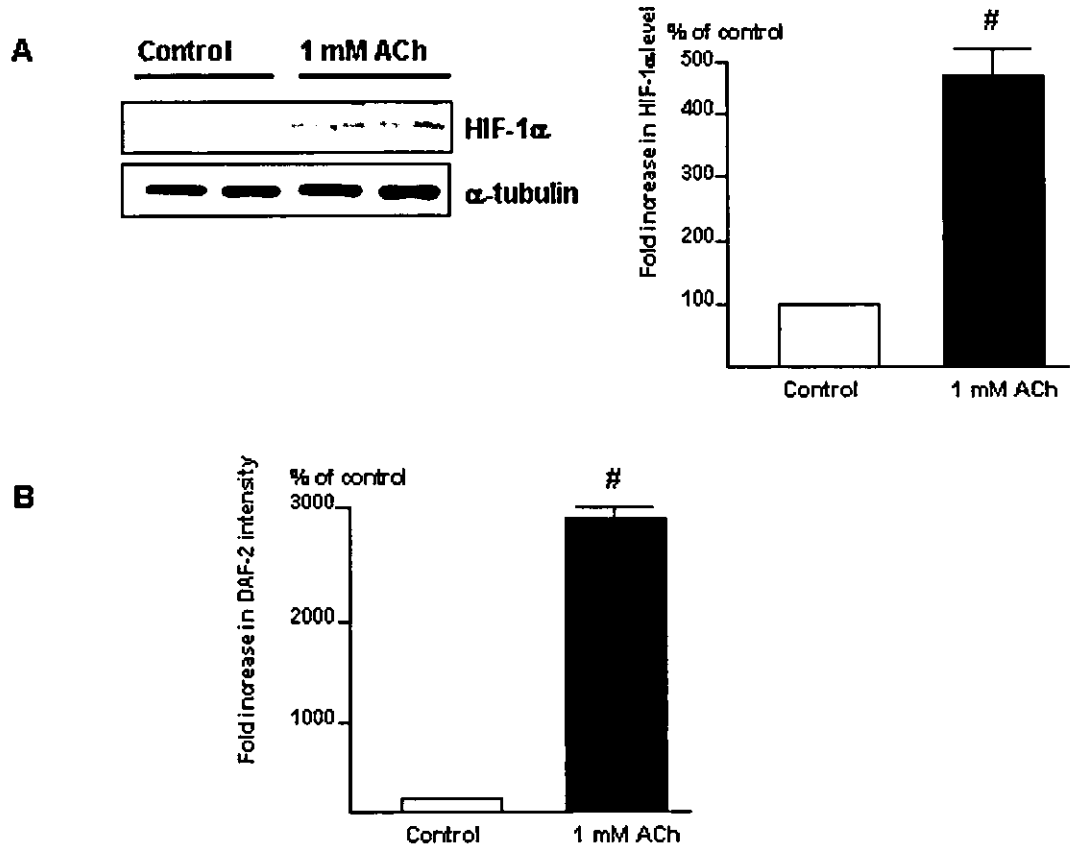

Figure 2

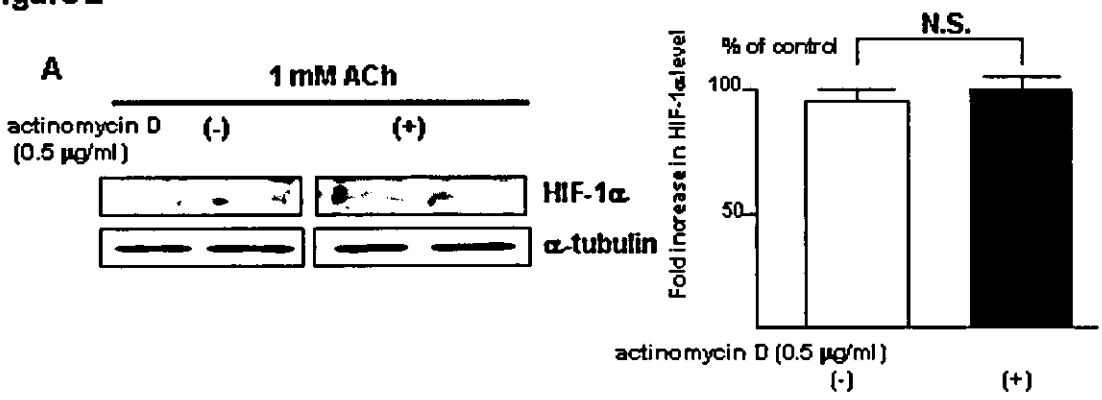

Kakinuma Y et al
Figure 2

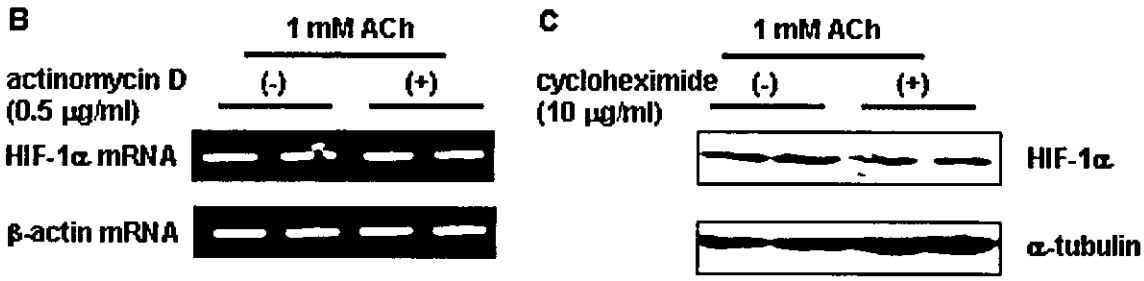

Figure 3

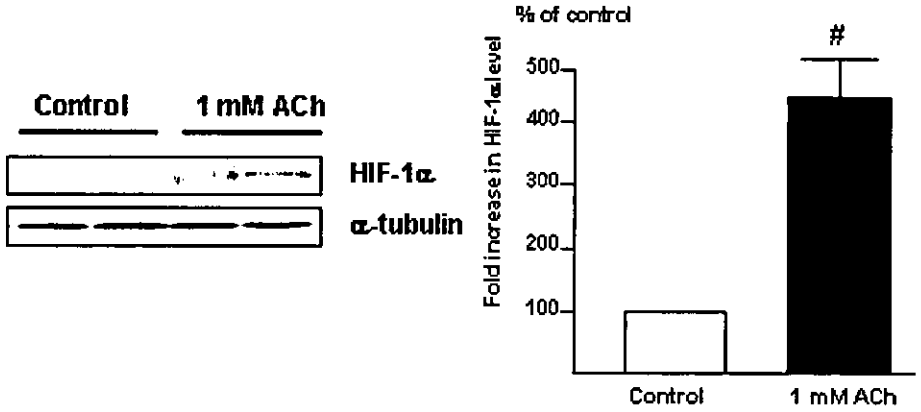

Figure 4

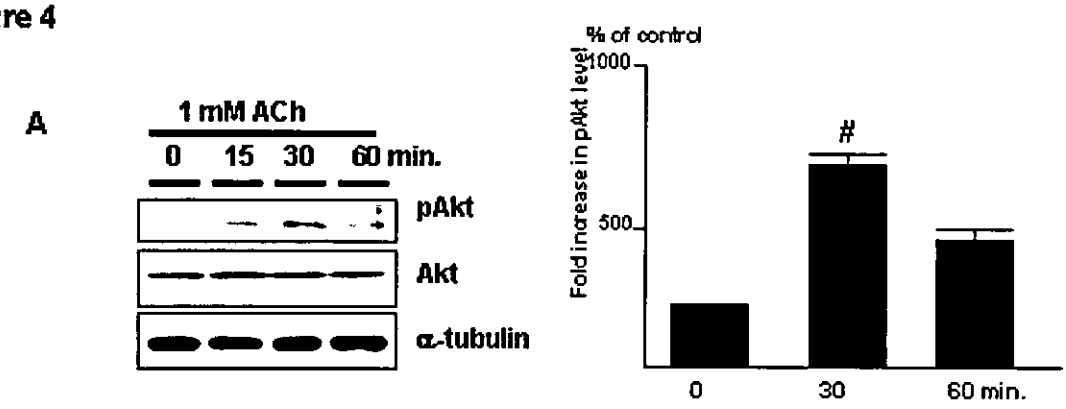

Kakinuma Y et al
Figure 4

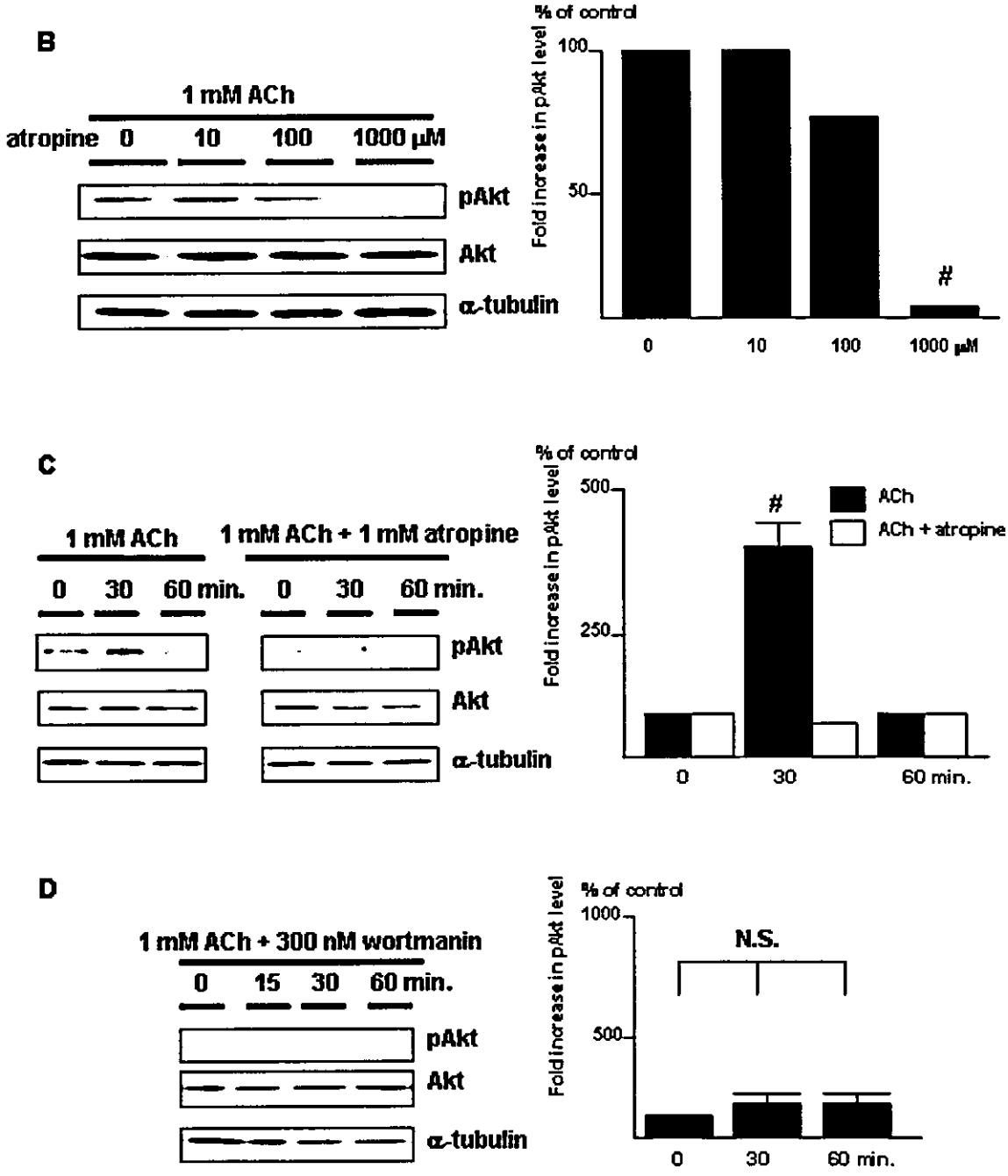

Kakinuma Y et al
Figure 4

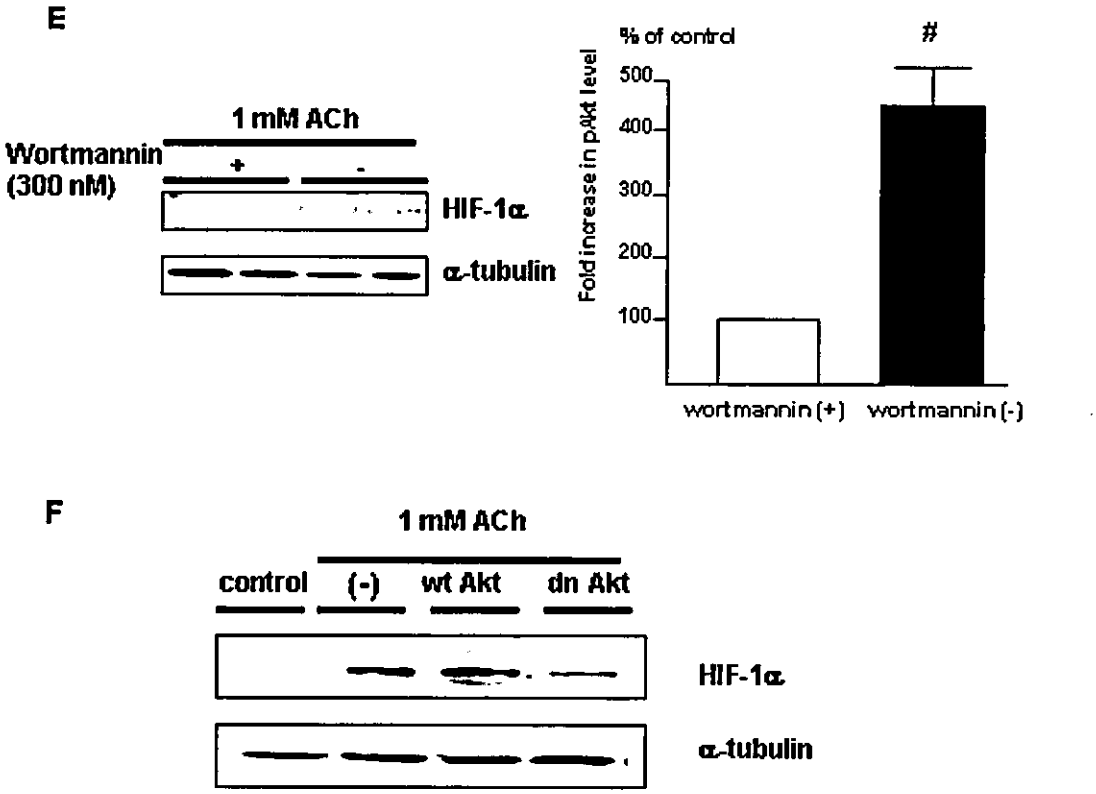

Figure 5

Kakinuma Y et al
Figure 5

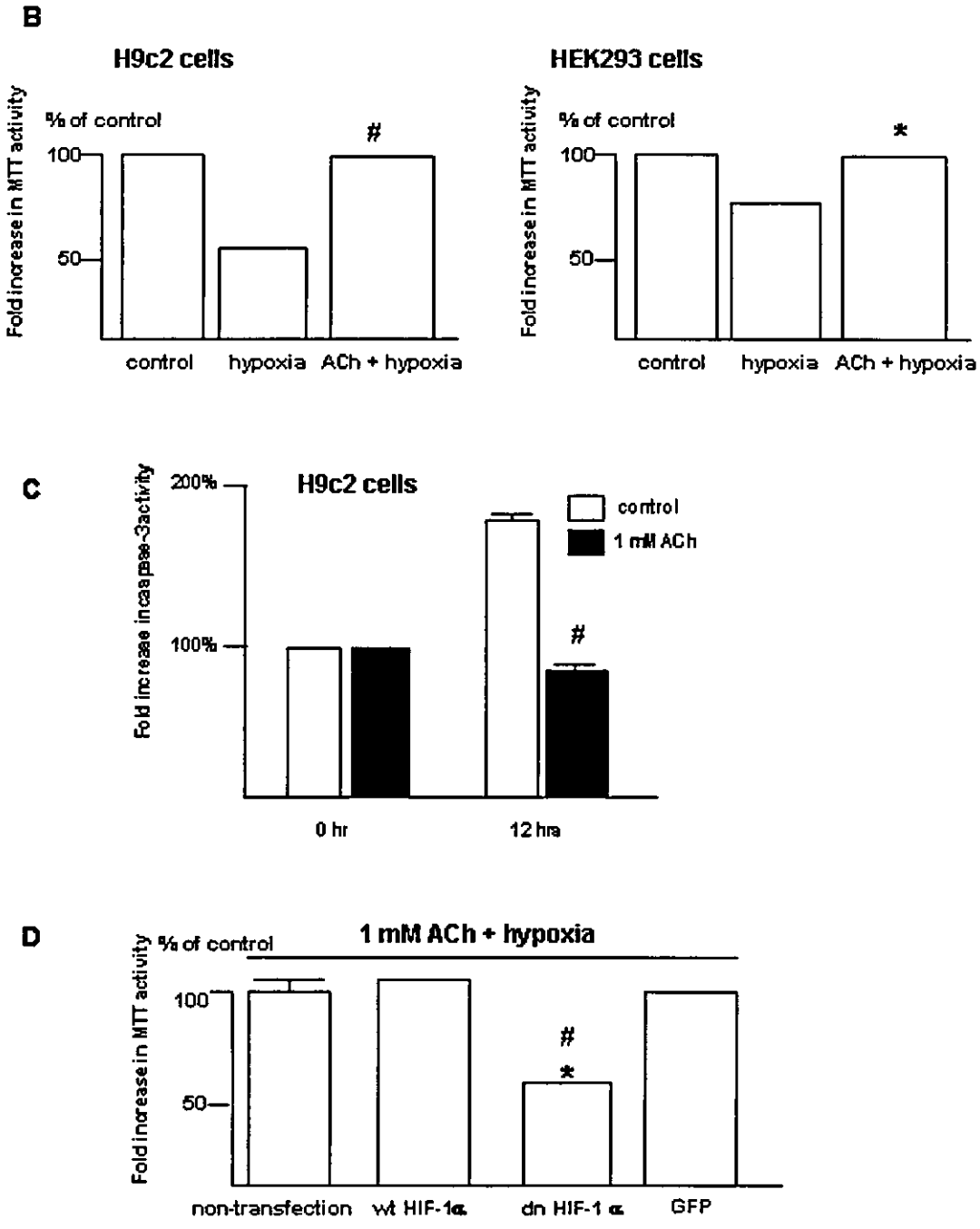

Kakinuma Y et al
Figure 6

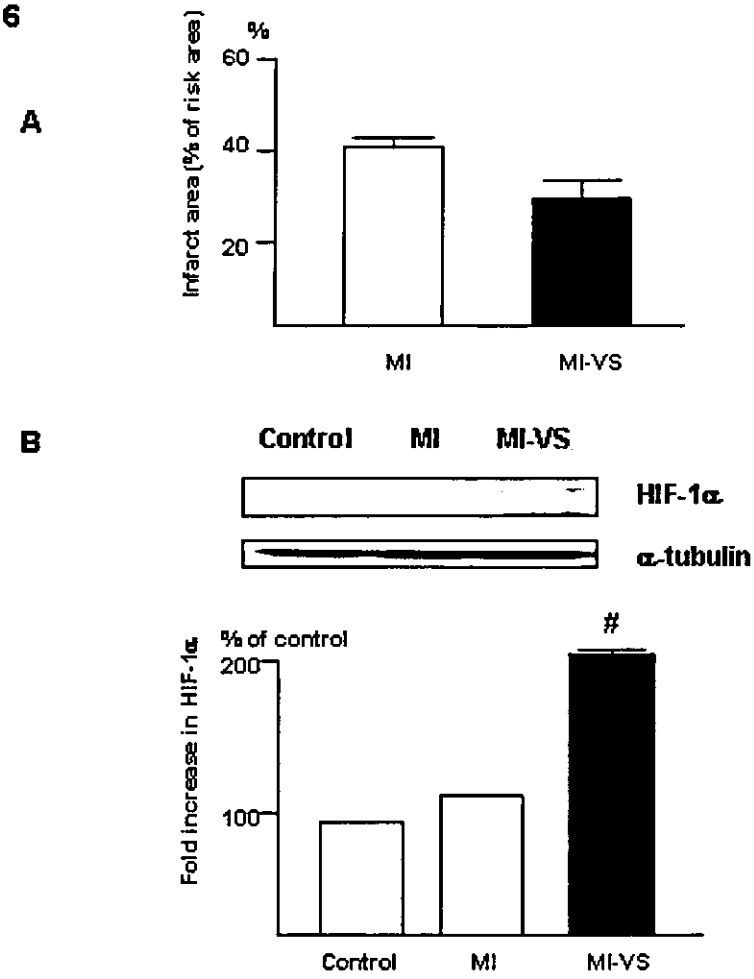

Figure 7

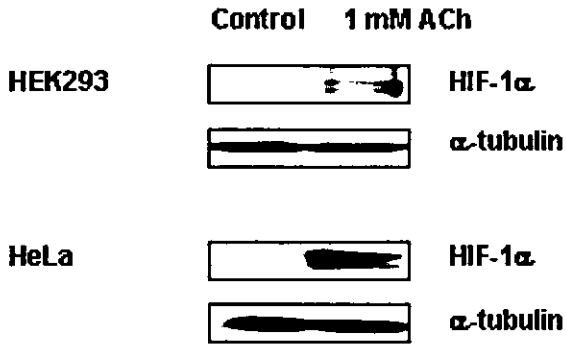

HIF-1α is Involved in the Attenuation of Experimentally Induced Rat Glomerulonephritis

Yoshihiro Kudo[1], Yoshihiko Kakinuma[2], Yasukiyo Mori[3], Norihito Morimoto[1], Takashi Karashima[4], Mutsuo Furihata[5], Takayuki Sato[2], Taro Shuin[4], Tetsuro Sugiura[1]

Departments of [1]Laboratory Medicine, [2]Cardiovascular Control, [4]Urology and [5] Tumor Pathology, Kochi Medical School, Kochi, Japan
[3]The Second Department of Internal Medicine, Kansai Medical University, Osaka, Japan

Address for Correspondence; Yoshihiko Kakinuma, M.D., Ph.D. Department of Cardiovascular Control, Kochi Medical School, Kochi 783-8505, Japan
Phone: +81-88-880-2311, Fax: +81-88-880-2310, E-mail: kakinuma@med.kochi-u.ac.jp

Abstract

Background/Aim: Among various kidney disease models, there are few rat glomerulonephritis (GN) models that develop in a short time, and with mainly glomerular lesions. Hypoxia-inducible factor (HIF)-1α is a transcriptional factor that induces genes supporting cell survival, but the involvement of HIF-1α in attenuating the progression of GN remains to be elucidated. We developed a new model of rat GN by co-administration of Angiotensin II (AII) with Habu snake venom (HV) and investigated whether HIF-1α is involved in renal protection. ***Methods:*** Male Wistar rats were unilaterally nephrectomized on day –1, and divided into 4 groups on day 0; N group (no treatment), HV group, A group (AII), and H+A group (HV and AII). To pre-induce HIF-1α, cobalt chloride ($CoCl_2$) was injected twice before injections of HV and AII in 11 rats.
Results: GN was detected only in the H+A group; observed first on day 2 and aggravated thereafter. HIF-1α was expressed in the glomeruli and renal tubules in the A and H+A groups. In the H+A group, GN was remarkably reduced by $CoCl_2$ pre-treatment (44.9% to 12.2%, $p<0.01$). ***Conclusion:*** Both HV and AII were critical for the development of GN, and HIF-1α remarkably attenuated the progression of GN.

Key Words

Glomerulonephritis, Habu snake venom, Angiotensin II, HIF-1α

Introduction

Many animal studies have been performed in attempts to overcome the poor prognosis of chronic renal failure due to diabetic nephropathy and glomerulonephritis (GN) [1-5]. Although factors involved in the pathogenesis of GN have been intensively investigated, the development of a proper animal GN model with high reproducibility and simplicity as well as a model without time-consuming process are required. Experimental rat models of GN are classified into several groups in terms of the pathophysiological mechanisms of renal diseases. Anti-glomerular basement membrane (GBM) nephritis was developed with depositions of immune complex using anti-glomerular basement membrane antibody [3,6], tubulo-interstitial injury was caused by cyclosporine A [4] and injury of renal tubules by ischemia [5]. However, there are few rat GN models with mainly pathological features in the glomeruli that are developed in a short time [7]. Angiotensin II (AII) is known to increase blood pressure through vascular contraction, and to be profoundly involved in vascular hypertrophy and the contraction of intrarenal arteries. AII is also directly involved in the progression of glomerulosclerosis via the effect of hyperfiltration with or without hypertension [8,9]. Many studies have revealed important factors involved in the pathogenesis of GN or factors aggravating GN, but evaluating further factors that suppress the occurrence of GN is also crucial. To investigate the features of renal protection, we focused on hypoxia-inducible factor (HIF)-1α. HIF-1α, a transcriptional factor with formation of a heterodimer with HIF-1β [10], is post-transcriptionally regulated and its protein level is elevated by hypoxia through inhibition of ubiquitin-mediated degradation. HIF-1α is known to be a survival factor responsible for inducing lines of genes supporting cell survival such as glucose metabolism (glucose transporters and glycolysis enzymes), vasomotor regulation (heme oxygenase-1 and endothelin-1), angiogenic growth (vascular endothelial growth factor), and anemia control (erythropoietin and transferrin) [11-13]. Recent studies have demonstrated that non-hypoxic stimuli like AII can also activate HIF-1α [14,15], but the role of HIF-1α induction in attenuating the progression of GN remains to be elucidated. Accordingly, we

developed a new rat GN model by co-administration of AII with Habu snake venom (HV) and investigated whether pre-induction of HIF-1α leads to renal protection.

Materials and Methods

Development of Rat GN Model

All experiments were approved by the institutional review board for the care of animal subjects and were performed in accordance with guidelines of Kochi Medical School. Nine-weeks old male Wistar rats (180-220g) were purchased from Japan SLC (Shizuoka, Japan). Rats were unilaterally nephrectomized on day -1. On day 0, the rats were divided into 4 groups. In the first group, no treatment was performed with any reagents or surgical procedure (N group, n=6). In the second group, rats were injected with 3.5 mg/kg of HV (Sigma-Aldrich Co., Steinheim, Germany) through the femoral vein (HV group, n=11). In the third group, rats were continuously administered with AII (100ng/min, Peptide Institute, Inc., Osaka, Japan) using Alzet osmotic pumps (DURECT Co., Cupertino, CA) (A group, n=11). In the fourth group, rats were administered with both HV and AII (H+A group, n=22). Rats were sacrificed on days 1, 2, 3 or 4, and kidneys excised for histochemical analysis (fig. 1).

Measurement of Systolic Blood Pressure

Systolic blood pressure (SBP) was measured by the tail-cuff method with an electro-sphygmomanometer (BP-98A, Softron Co., Tokyo, Japan). SBP was measured in conscious rats every day from day -1 to day 2. The SBP value for each rat was calculated as the average of 3 separate measurements at each session. SBP measurement was performed between 9 and 12 a.m. by a single blinded investigator.

Measurements of Serum Urea Nitrogen and Creatinine

Before the sacrifice, blood samples were obtained via an axillary vein for determination of serum urea nitrogen (UN) and creatinine (Cr) levels. Serum UN and Cr levels were determined enzymatically with automation-analysis equipment (Hitachi 7350, Hitachi Co., Ibaragi, Japan) in our laboratory center.

Histological Analysis

To evaluate the progression of GN in our animal model, histological analyses were performed using the periodic acid-Schiff (PAS) and periodic acid-methenamine silver (PAM) reagents. After the specimens were paraffin-embedded, 4-micrometer sectioned samples were stained with PAS and PAM reagents and counterstained with hematoxylin. For quantitative analysis, the ratio of damaged glomeruli to all glomeruli in the sectioned sample was calculated and the percentage of GN in the section was evaluated. Moreover, semiquantitative analysis was performed to evaluate more precisely the morphological changes of our GN model according to the protocol in previous studies [16,17]. A minimum of 20 glomeruli (ranging from 20 to 60 glomeruli) in each specimen were examined and the severity of the mesangiolysis lesion was graded from 0 to 4+ according to the percentage of glomerular involvement; a 1+ lesion represented an involvement of 25 % of the glomerulus while a 4+ lesion indicated that 100 % of the glomerulus was involved. Thus, the mesangiolysis score (MES) was then obtained by multiplying the degree of damage (0 to 4+) by the percentage of the glomeruli with the lesion. Tubular injuries including tubular necrosis or occlusion of collecting ducts by cast material were graded as mild (1+), moderate (2+), or severe (3+).

Western Blot Analysis

Nuclear protein from whole kidney was prepared using NE-PER Nuclear and Cytoplasmic Extraction Reagents (Pierce Biotechnology, Inc. Rockford, Illinois, USA). Nuclear protein was electrophoresed using 10% SDS-PAGE gels and transferred to polyvinylidene difluoride membrane (Immobilon-P, Millipore Co., Bedford, Massachusetts, USA). A monoclonal IgG HIF-1α antibody α67 (Novus Biological, Littleton, Colorado, USA) was used; a horseradish peroxidase-conjugated antibody (Promega Co., Madison, USA) was used as a secondary antibody. The ECL Western blotting systems (Amersham Bioscience, Upsala, Sweden) was used for detection.

Immunohistochemical Analysis

Paraffin sections including the samples were dewaxed in xylene and rehydrated in a series of ethanol, and then washed in distilled water before staining procedures. According to the instruction provided by the manufacturer, HIF-1α was identified with rabbit polyclonal anti-HIF-1α antibody H-206 (Santa Cruz Biotechnology, California, USA) utilizing the catalyzed signal amplification system (Dako, Hamburg, Germany) based on the streptavidin-biotin-peroxidase reaction. Antigen retrieval was performed for 5 min in a preheated Dako target retrieval solution using a microwave. Incubation procedures were performed in a humidified chamber. Following the incubation, specimens were washed 3 times in TBST buffer. The specificity of staining was confirmed by substitution of the primary antibody for a normal rabbit IgG and additionally by an immunohistochemical reaction without a primary antibody but with the secondary antibody alone.

An Experiment using Cobalt Chloride as a Pretreatment

Rats were twice subcutaneously administered 30mg/kg of cobalt chloride ($CoCl_2$) at a 12 hour interval ($CoCl_2$ group) (n=11), followed by unilateral

nephrectomy. Then, the rats were administered with HV and AII. As a comparison, rats were injected with 0.9% NaCl solution instead of $CoCl_2$, followed by the same protocol as the $CoCl_2$ group (n=11). After $CoCl_2$ administration, however, before injection of HV and AII, a kidney was excised as a sample to examine expression level of HIF-1α ($CoCl_2$ Pre). Likewise, 2 days after administration of HV and AII, a kidney was also excised ($CoCl_2$ Day2). To compare the expression level of HIF-1α by $CoCl_2$ before GN and the severity of pathology of GN, we investigated whether pre-induction of HIF-1α. is involved in renal protection.

Statistical Analysis

Data are reported as mean ± SEM. A paired *t* test was used for paired samples and Student's *t* test was used to compare the 2 groups. One-way layout analysis of variance or repeated measures of analysis of variance were used to compare multiple groups. If the p value was significant, Scheffe's multiple comparison was performed. A p value < 0.05 were considered significant.

Results

AII combined with HV developed GN

Morphological studies using PAS and PAM staining revealed that there are no glomerular or tubular injuries in N group (fig. 2A), HV group (fig. 2B), A group (fig. 2C), however, GN was detected only in the H+A group (fig. 2E). Although renal tubular casts were observed, glomerular changes were scarcely observed on day 1 after AII and HV administration (figs. 2D, 3). GN was initially detected on day 2 (figs. 2E, 2F, 3), followed by further aggravation during the time course (data not shown). Renal tubular injury including tubular necrosis was not remarkable, and extensive cellular infiltration was not found in the interstitial regions (fig. 3). On the other hand, characteristic focal and segmental mesangiolysis, explained as capillary aneurysmal ballooning, was observed with dilatation of glomerulus (figs. 2E, 2F). The rate of occurrence of GN on day 2 was 44.9±2.6 %, and the MES score of the H+A group was 199±15 (fig. 3). On the other hand, in the HV group, less than 2 % had morphologic changes of mesangiolysis during 4 days, and the MES score was 10±5 (figs. 2B, 3). Moreover, in the A group, there were no morphologic changes during the time course (fig. 2C).

Changes in serum UN and Cr

Serum UN and Cr were 18.4±0.7, 0.31±0.01 mg/dl, respectively, on day 2 in the N group. In the H+A group, serum UN and Cr levels increased to 41.5±4.0, 0.57±0.05 mg/dl, respectively, on day 2; significantly higher than those in the N group (figs. 4A, 4B). In contrast, serum UN and Cr levels in the H+A group on day 1 (24.0±1.8 and 0.42±0.02 mg/dl, respectively) were similar to the level of the N group. There were no significant differences in serum UN and Cr level among the HV, A and N groups.

SBP response

SBP values of each group are shown in figure 4C. There were no significant differences in SBP after nephrectomy among the 4 groups. Administration of AII caused a significant increase of SBP on day 1 (186±4 mmHg) and persisted to day 2 (192±1 mmHg). SBP in the H+A group on day 2 (183±3 mmHg) was comparable to that in the A group. Administration of HV had no influence on SBP during the 2 days.

Expression Level of HIF-1α Protein

Western blot analysis revealed that the expression level of HIF-1α protein increased in the H+A and A groups (fig. 5A), compatible with the results of immunohistochemical analysis. Expressions of HIF-1α protein were observed in the A and H+A groups, but protein expression was not detected in the N and HV groups. These data suggest that HIF-1α was induced mainly by AII, and, at least in part, was related to the pathogenesis of GN or to the defense mechanism against the progression of GN.

Induction of HIF-1α in Glomeruli and Renal Tubules

Immunohistochemical study demonstrated positive nuclear staining of HIF-1α in glomeruli, renal tubules (figs. 2I, 2J), collecting ducts and epithelium of the papilla (data not shown) in the A and H+A groups. In contrast, no positive nuclear signals were detected in the N (fig. 2H) and HV (data not shown) groups. HIF-1α positive cells were mainly detected in mesangial cells in glomeruli (figs. 2I, 2J). As demonstrated, especially in the H+A group (fig. 2J), HIF-1α was expressed in the intact part of the glomerulus, but not in the injured part of the same glomerulus. Furthermore, nuclear HIF-1α positive signals were observed in smooth muscle cells in peripheral renal arteries (data not shown).

$CoCl_2$ Pretreatment Inhibits the Progression of GN

To further investigate whether HIF-1α is involved in the development of nephropathy or in the anti-progressive action, we pretreated rats with $CoCl_2$. As demonstrated in fig. 5B, pretreatment with $CoCl_2$ increased HIF-1α expression before administration of HV and AII (Pre-1), suggesting that HIF-1α was induced by $CoCl_2$ before development of GN. Even on day 2, the expression level of HIF-1α was increased in the $CoCl_2$ group ($CoCl_2$ Day2-1). In the $CoCl_2$ group, focal mesangiolysis with glomeruli enlargement was still observed, but the number of GN was much less than in those without $CoCl_2$ pretreatment (fig. 2G).

Thus, 7 of 11 rats (63.6%) with $CoCl_2$ pretreatment were rescued from GN alone, while the other 4 (36.4%) were not; showing a comparable severity level of GN with the non-$CoCl_2$ group. As

demonstrated in fig. 5B, unlike Pre-1, Pre-2 did not induce HIF-1α with $CoCl_2$ and showed no $CoCl_2$ suppression of GN. The ratio between rats rescued or not-rescued from GN was comparable with that between pre-induction and non-induction of HIF-1α by $CoCl_2$, as demonstrated in fig. 5C. In the $CoCl_2$ group the rate of GN from each rat decreased to 12.2±2.1%, which was in great contrast to 44.9±2.6% in the non-$CoCl_2$ group. Furthermore, serum UN and Cr levels on day 2 were significantly lower in the $CoCl_2$ than in the non-$CoCl_2$ group ($p<0.05$) (figs. 6A, 6B), despite comparable SBP values between the 2 groups (fig. 6C).

Discussion

In this study, we developed a new model of GN induced by both HV and AII. This model has several distinct characteristics. First, GN developed rapidly, and was detected on the second day after administration of HV and AII. Many models of GN have been reported including 5/6 nephrectomized and Thy-1.1 nephritis models [18,19]. However, these models take a long time to develop nephropathy. In contrast, our protocol induced GN in 2 days, suggesting that one of the advantages our model has over others is in terms of the time course. Further, pathological findings were restricted to glomerular regions without remarkable tubular or interstitial lesions. Since our GN model developed within 2 days, our model also has advantages for disclosing the specifically critical time point of the development of GN. Further, the development rate of GN was almost 100%, indicating the high reproducibility of our model. This basis of the rat model was initially developed by Barnes JL et al. who reported that the progression of AII-induced renal injury was accelerated by preexisting injury induced by HV [20]; ours, which now optimizes the reproducibility of GN, is a modification of their model.

Habu induced nephropathy was reported to develop within 1 day by a dose of 2.0-4.0 mg/kg HV (in our model 3.5 mg/kg) and the main pathological change was "mesangiolysis" [21,22]. However, for reasons we haven't as yet ascertained, in our study no rats showed Habu-nephropathy specific pathological findings during the first week in the HV group. On the other hand, AII is one of the major factors responsible for the pathogenesis of GN, because it remarkably increases glomerular pressure causing hyperfiltration, production of extracellular matrix and expression of lines of genes involving GN [23-25]. Further, since AII has some ischemic effects on kidney, there is the possibility that an AII-induced ischemic effect causes the GN depicted in our model. However, as demonstrated in this study, glomerular injury was predominantly observed, and was not associated with renal tubular lesions, i.e., tubular necrosis suggesting renal ischemia. Therefore, in accordance with the pathological characteristic of this GN, AII-induced renal ischemia may not be responsible for the development in our model. Additionally, in this study, SBP increased in the A and A+H groups, but GN was not induced in the A group. Therefore, GN in our model was induced not by HV or AII alone, but by the combination of HV and AII, independent of any increase in systemic blood pressure.

HIF-1α is a master transcriptional factor, transactivating the expression of many genes important for cell survival under hypoxic conditions [11-13,26]. These genes are responsible for glycolysis, angiogenesis, proliferation and iron metabolism, all of which are induced by hypoxic stress; thus, the induction of HIF-1α is a marker of hypoxia. HIF-1α is regulated at the post-translational level by the proteasome system through ubiquitination with von Hippel Lindeau (VHL) protein [27,28]. As previously reported, this regulation of HIF-1α protein level is dependent on the concentration of oxygen. Hypoxia induces enhancement of HIF-1α protein stability leading to the elevation of the protein level due to inhibition of degradation by VHL. Therefore, hypoxia induces adaptation in cells including induction of HIF-1α; the hypoxic pathway. On the other hand, a line of evidence has recently accumulated that suggests that HIF-1α is also regulated independent of oxygen concentration through the non-hypoxic pathway [14,15]. AII is reported to regulate HIF-1α both at transcriptional and post-translational levels in vascular smooth muscle cells cultured under normoxic condition through the AII type 1 receptor [14,15]. Moreover, HIF-1α is also post-translationally regulated in several cell lines in the presence of tumor necrosis factor-α or nitric oxide independent of oxygen contents [29,30].

As demonstrated in this study, immunoreactivity of HIF-1α was not detected in the N group (no treatment group), but HIF-1α was detected in the nuclei of glomerular, tubular and epithelium cells of the papilla by administration of AII alone or AII and HV together. This is the first evidence showing that HIF-1α was detected in the kidney by AII, independent of systemic hypoxic stress. As indicated here, HIF-1α was found to be expressed only in intact, not damaged glomeruli. Even within a glomerulus, only the intact part of glomerular cells expressed HIF-1α. Considering the fact that induction of HIF-1α is one of the defense mechanisms for cell survival [31-33], our data indicate that induction of HIF-1α is a marker of glomeruli survival; indeed, it could be a marker of renal protection.

To further investigate whether HIF-1α is involved in the progression or protection of GN, pre-induction of HIF-1α was performed with $CoCl_2$ before administration of HV and AII. Surprisingly, the induction of HIF-1α by $CoCl_2$ pretreatment